CHEMISTRY
A EUROPEAN JOURNAL

DOI: 10.1002/chem.200600467

Fluorogenic 1,3-Dipolar Cycloaddition within the Hydrophobic Core of a Shell Cross-Linked Nanoparticle

Rachel K. O'Reilly,[a, b, d] Maisie J. Joralemon,[a, e] Craig J. Hawker,*[b, c] and Karen L. Wooley*[a]

Abstract: Using either nitroxide mediated polymerization (NMP) or reversible addition fragmentation transfer (RAFT) techniques, novel block copolymers that present terminal acetylenes, in the side chain of the styrenic block, were obtained with narrow polydispersities and targeted molecular weights. For the conversion of these acetylene-functionalized polymers to amphiphilic block copolymers, RAFT techniques were preferred. Mild protection/deprotection chemistries were employed which were compatible with the incorporation of the acetylene functionality in the hydrophobic segment. These acetylene-functionalized, Click-readied amphiphilic block copolymers were then self-assembled and cross-linked to afford shell cross-linked knedel-like (SCK) nanoparticles that contained acetylene groups in the core domain. The hydrodynamic diameters (D_h) of the block copolymer micelles and nanoparticles were determined by dynamic light scattering (DLS), and the dimensions of the nanoparticles were characterized using tapping-mode atomic force microscopy (AFM) and transmission electron microscopy (TEM). The chemical availability of the Click functionality within the core domain of the SCKs was investigated using the copper(I)-catalyzed 1,3-dipolar fluorogenic cycloaddition with a non-fluorescent 3-azidocoumarin profluorophore to afford intensely fluorescent nanoparticles.

Keywords: block copolymers · click chemistry · fluorogenic · nanostructures

Introduction

The supramolecular self-assembly of amphiphilic block copolymers into polymeric micelles, with a core-shell type structure, in aqueous solution has received much interest over the last decade, due to their effectiveness as drug delivery vehicles or as nanoreactors.[1–10] These micelles are of interest for drug delivery systems, as the hydrophobic core of the micelles can behave as a carrier compartment that encapsulates a lipophilic molecule and allows for the water solubility limits of hydrophobic drugs to be exceeded. The hydrophilic shell, which consists of a brush-like protective corona, stabilizes the micelles in aqueous solution and protects the contents of the hydrophobic core from hydrolysis or degradation. The cross-linking of micelles in the core or shell domain to afford robust nanoparticles imparts stabilization and also improves the temporal control of micelles as drug delivery carriers. An important advantage of amphiphilic block copolymers for drug delivery applications is the ability to tailor the relative ratio of block lengths, total molecular weight and composition, which allows for control over the size and morphology of the resulting micelles and nanoparticles.[11–18]

[a] Dr. R. K. O'Reilly, Dr. M. J. Joralemon, Prof. K. L. Wooley
Washington University in Saint Louis
Center for Materials Innovation and Department of Chemistry
One Brookings Drive, St. Louis, MO 63130-4899 (USA)
Fax: (+1) 314-935-9844
E-mail: klwooley@artsci.wustl.edu

[b] Dr. R. K. O'Reilly, Prof. C. J. Hawker
IBM Almaden Research Center, 650 Harry Road
San Jose, CA 95120 (USA)
E-mail: hawker@chem.ucsb.edu

[c] Prof. C. J. Hawker
Materials Research Laboratory, University of California
Santa Barbara, CA 93106 (USA)
Fax: (+1) 805-893-8797

[d] Dr. R. K. O'Reilly
Current Address:
The University Chemistry Laboratory, Cambridge University
Lensfield Road, CB2 1EW, Cambridge (UK)

[e] Dr. M. J. Joralemon
Current Address:
Department of Polymer Science and Engineering, University of Massachusetts
Conte Center for Polymer Research, Amherst, MA 01003 (USA)

To enable the construction of well-defined, functional amphiphilic block copolymers, for applications in the emerging field of nanotechnology, controlled routes to their synthesis and functionalization must be developed, and controlled radical polymerization (CRP)[19–22] has proven to be the favored mechanism. One of the most versatile methods of CRP is reversible addition fragmentation chain transfer (RAFT) polymerization.[23,24] RAFT has enabled the synthesis of complex architectures, including block copolymers, dendrimers, and star structures of targeted molecular weights and low polydispersities.[25–28] An important feature of RAFT polymerization is that the chain transfer agent is the chain-end functionality, and allows for the subsequent polymerization of other monomers to form block copolymers. Moreover, the unprecedented flexibility of RAFT allows the polymerization of a diverse range of monomers, including (meth)acrylates, styrenes, and acrylamides, under relatively mild polymerization conditions.[24,29–35]

In general, with the introduction of appropriate functionalities into selective regions within the nanostructures, it is possible to tailor the nanoparticles and micelles for enhanced performance toward both higher selectivity and loading for drug targeting, among other applications.[36] In this fundamental study, therefore, nanoparticles were designed and synthesized to present Click-readied functionalities throughout the core region, which were then probed as possible therapeutic and imaging agent attachment sites via reaction with the profluorophore 3-azidocoumarin. Click chemistry is a modular synthetic approach that couples an acetylene and azide via a regioselective 1,3-dipolar cycloaddition reaction in the presence of a copper catalyst, to afford a 1,4-disubstituted 1,2,3-triazole ring.[37–40] This Click reaction is highly specific, thus leading to facile purification and has been found to proceed with quantitative yield in both protic and aprotic media.[41–45] Furthermore, azides and acetylenes are relatively inert and are compatible with the functionalities of bio(macro)molecules, thus enabling their application in a wide range of environments,[46–56] and lend this Click chemistry towards employment for the covalent attachment of ligands to nanoparticles. This type of reaction has previously been utilized to covalently attach biomolecules and labeling molecules to copolymers, micelles and nanoparticles.[57–59]

This study utilizes 3-azidocoumarin as a profluorophore, due to its biocompatibility and its literature precedent as a probe for the ligation of a library of small molecules.[60,61] It was previously demonstrated that substitutions at the 3- and 7-positions of coumarin dyes have a profound impact on the electronic structure and, thereby, the associated fluorescent properties.[62,63] Wang and co-workers recently reported 3-azidocoumarin shows no fluorescence, due to the quenching effect of the electron rich α-nitrogen of the azido group.[61] It was also demonstrated that a fluorescent signal can be triggered by the Click reaction upon formation of a triazole ring between the 3-azidocoumarin and acetylene-functionalized small molecule, due to the resulting alteration of the electronic structure. Thus, in this study we examined the fluorogenic reaction between a 3-azidocoumarin and acetylene functionality located within the hydrophobic core domain of a SCK nanoparticle, to allow for the confirmation that the hydrophobic 3-azidocoumarin both migrated into the SCK core and underwent covalent Click attachment of the coumarin within the nanoparticle rather than sequestration alone. The results presented demonstrate the ability to conduct a combination of supramolecular and covalent chemistry within the confines of a well-defined and robust nanoscale object.

Results and Discussion

The general strategy began with the preparation of amphiphilic block copolymers carrying reactive side chain substituents along a specific region of the backbone, and was followed by their supramolecular assembly in aqueous solution, cross-linking stabilization reactions, and finally determination of the availability and reactivity of the reactive substituents. CRP techniques were used for the growth of a diblock copolymer comprised of an acrylate block segment and a styrene block segment that also included protected acetylene functionalities. Simultaneous deprotection of the acrylate block and removal of the acetylene protecting group then afforded the Click-readied amphiphilic diblock copolymers. The synthesis of these amphiphilic block copolymers having acetylene side chain groups along the hydrophobic chain segment, their self-assembly, and cross-linking to afford acetylene core-functionalized SCKs, as well as the subsequent Click reaction within the core of these SCKs with a fluorogenic probe, are each described within the sections below.

Synthesis of acetylene-functionalized amphiphilic block copolymers: For the synthesis of acetylene-functionalized amphiphilic block copolymers, careful selection of protection and deprotection chemistries were critical. We have recently demonstrated that the instability of the acetylene moieties towards conditions employed for *tert*-butyl ester deprotection and the incompatibility between functionalization chemistries prevented successful acetylene incorporation, previously, within the hydrophobic segment of poly(acrylic acid)-*b*-polystyrene (PAA-*b*-PS) block copolymers.[57] In addition, literature results indicated that the acetylene functionality was not chemically or thermally stable under the conditions required for controlled polymerization, and thus protection was provided by a trimethylsilyl (TMS) group.[64–67] It also has been demonstrated that the TMS protecting group could be removed post-polymerization in quantitative yields using tetrabutylammonium fluoride (TBAF) to afford the acetylene styrene-functionalized copolymers.[68] The controlled NMP of protected acetylene styrenic monomers has received recent attention also by Grubbs and co-workers for applications in the preparation of cobalt nanoparticles.[69,70]

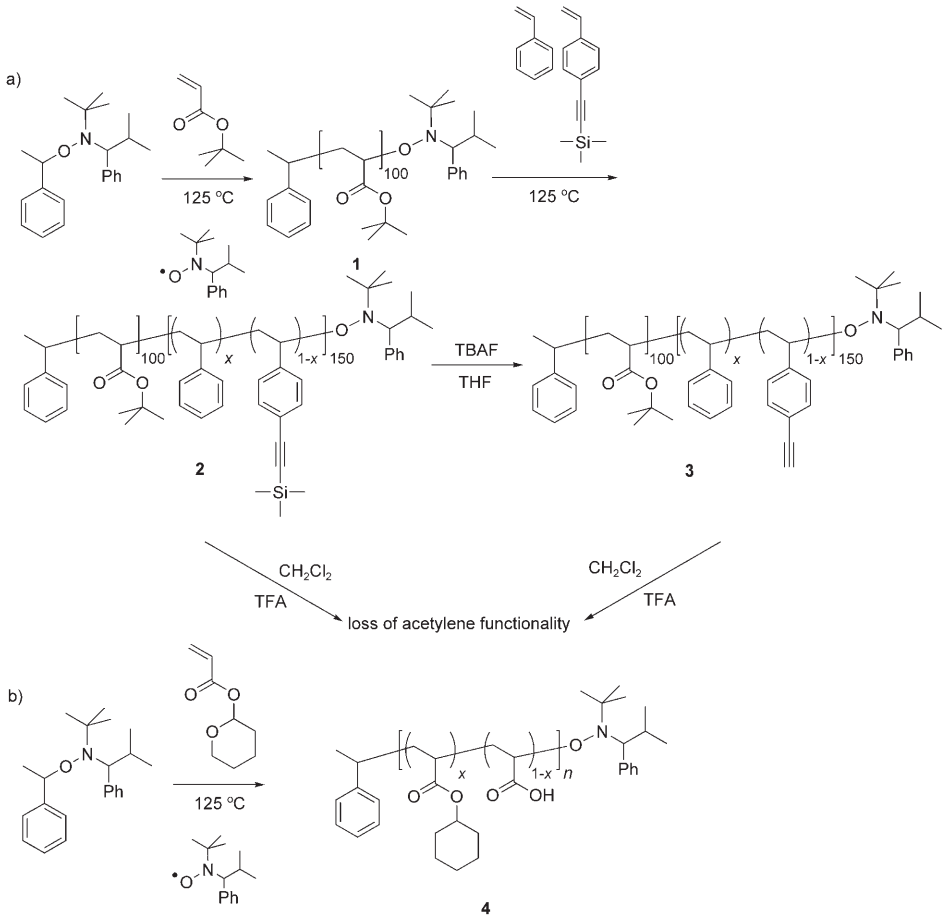

Scheme 1. a) Synthesis of P*t*BuA-*b*-[PS-*co*-PSC≡CTMS] block copolymer using NMP and subsequent deprotection strategies. b) Attempted synthesis of PTHPA using NMP, but with complications from unwanted thermal deprotection.

Initial routes toward the incorporation of TMS acetylene groups within the styrenic domain of PAA-*b*-PS block copolymers investigated the NMP of *tert*-butyl acrylate (*t*BuA), the alkoxyamino-terminated poly(*tert*-butyl acrylate) (P*t*BuA, **1**: $M_n = 13\,000\ g\,mol^{-1}$, $M_w/M_n = 1.17$) from which was then utilized as a macroinitiator for the growth of a statistical styrene (S) and 4-(trimethylsilylethynyl)styrene (SC≡CTMS) block (Scheme 1a) (**2**: $M_n = 32\,000\ g\,mol^{-1}$, $M_w/M_n = 1.24$).[19] However, all attempts to deprotect the *tert*-butyl ester functionalities of **2**, to afford amphiphilic block copolymers, **3**, resulted in the loss of acetylene functionality (as evidenced by IR spectroscopy and the loss of absorbance at ca. 2160 cm^{-1}), even in the presence of the TMS protecting group.[71] It was determined that due to the relatively harsh conditions required for complete deprotection of the *tert*-butyl ester groups, other protection strategies for the acrylic acid segment should be investigated.

Tetrahydropyran (THP) was selected as an alternative protecting group for the acrylic acid functionality due to the ease of removal under either mild acidic conditions and/or heat.[72,73] Tetrahydropyran acrylate (THPA) has been polymerized previously using group transfer and radical polymerization techniques[74,75] and the sensitivity of PTHPA towards acid-catalyzed decomposition to PAA has enabled its use in chemically-amplified photosensitive coatings for applications in microlithography.[76–78] THPA was synthesized via literature methods and was polymerized as illustrated in Scheme 1b by using NMP.[79] Due to high temperatures required for NMP (ca. 100 °C) a significant degree of deprotection to PAA (ca. 40 %) was observed by IR spectroscopy (evidenced as a broad signal at 3500–3000 cm^{-1} and the appearance of a second carbonyl band at ca. 1710 cm^{-1}). In addition, the crude ^{1}H NMR spectrum (Figure 1) of **4** illustrated the presence of vinylic proton signals attributable to acrylic acid and also highlighted the presence of alkenyl protons assigned to dihydropyran, the small molecule formed on deprotection. Thus, alternative CRP techniques were investigated, that would allow for controlled polymerization of THPA with little or no deprotection.

In order to synthesize well-controlled THPA polymers and copolymers at lower polymerization temperatures, RAFT techniques were investigated, due to the high level of control that has been achieved previously in the polymerization of acrylates under relatively mild RAFT conditions. The RAFT agents utilized in this study are those reported recently by Perrier and co-workers for the polymerization of styrene, (meth)acrylates and acrylates.[80] Polymerization of THPA was performed at 70 °C using azobisisobutyronitrile (AIBN) as a radical initiator (Scheme 2). IR and ^{1}H NMR spectroscopic analyses indicated that the degree of ester deprotection was low (ca. 2 %) and GPC analysis confirmed that the polymer, **5**, was well-defined ($M_n^{GPC} = 8300\ g\,mol^{-1}$, $M_w/M_n = 1.18$). This polymer was then employed as a macroinitiator for growth of a statistical copolymer segment of styrene and 4-(trimethylsilylethynyl)styrene under similar polymerization conditions, except with the addition of benzene as a co-solvent, to afford $PTHPA_{50}$-*b*-[PS-*co*-PSC≡CTMS]$_{60}$ copolymer, **6**, ($M_n^{GPC} = 16\,200\ g\,mol^{-1}$, $M_w/M_n = 1.15$) with little or no deprotection observed by IR or ^{1}H NMR spectroscopic analyses (Figure 2). The signal characteristic of the methyl proton resonance of the TMS group appeared at about 0.20 ppm with reasonable integration ratios to the other signals from the remainder of the block

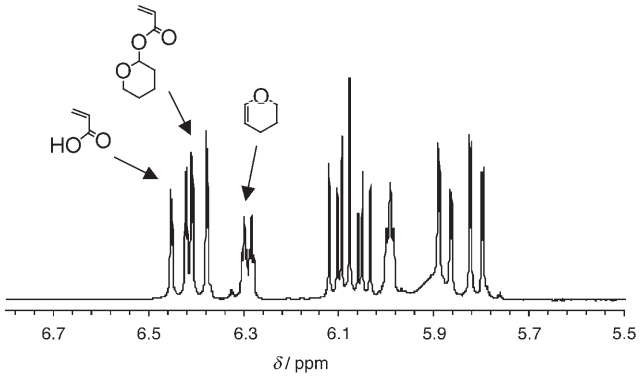

Figure 1. Crude ^{1}H NMR spectrum (300 MHz, $CDCl_3$) of the attempted NMP of THPA, illustrating deprotection of the ester functionalities of remaining monomer and the production of dihydropyran.

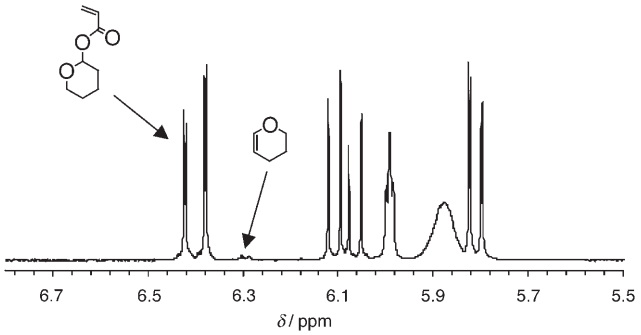

Figure 2. Crude ^{1}H NMR spectrum (300 MHz, $CDCl_3$) of the RAFT polymerization mixture on going from **5** to **6**, illustrating retention of the THP protecting groups.

copolymer protons, indicating that no cleavage of the silicon–carbon bond had occurred.

The simultaneous removal of both the THP and TMS functionalities was achieved in a single step using mild acidic conditions.[81,82] The quantitative removal of the TMS protecting group was ascertained by ^{1}H and ^{13}C NMR spectroscopic analyses, which showed the disappearance of the resonances at about 0.2 ppm (^{1}H NMR) and 0.4 ppm (^{13}C NMR) characteristic of the methyl protons and carbons of the TMS group. New resonance signals for the acetylene proton and carbon appeared at about δ 2.95 ppm (^{1}H NMR) and 83.8 and 77.3 ppm (^{13}C NMR). In addition, complete removal of the THP protecting groups was confirmed by IR and NMR spectroscopies and was supported by DSC analysis. This synthetic strategy allowed for the successful introduction of acetylene functionality into the hydrophobic chain segment of the amphiphilic diblock copolymer, **7**.

It was determined that the order in which the THPA and styrenic monomers were polymerized by RAFT was important to ensure that controlled polymerizations resulted in the preparation of a well-defined PTHPA-*b*-[PS-*co*-PSC≡CTMS] diblock copolymer. Attempts to first polymerize the styrenic block and then chain extend with the acrylate monomer gave polymers having bimodal molecular weight distributions, as had been observed similarly under NMP conditions.[83]

Synthesis of SCKs: Preparation of the acetylene core-functionalized SCKs involved the supramolecular assembly of **7** into micelles in aqueous solution, followed by covalent cross-linking via amidation reactions between acrylic acid residues in the micelle shell with diamine cross-linking agents (Scheme 3). The micellar organization of these linear amphiphilic polymer chains, **7**, was performed by addition of an equal volume of water to a solution of the diblocks in tetrahydrofuran (THF). Following extensive dialysis of the micelle solution, **8**, against water, a fraction of the PAA groups were cross-linked (nominally 50%), by using previously es-

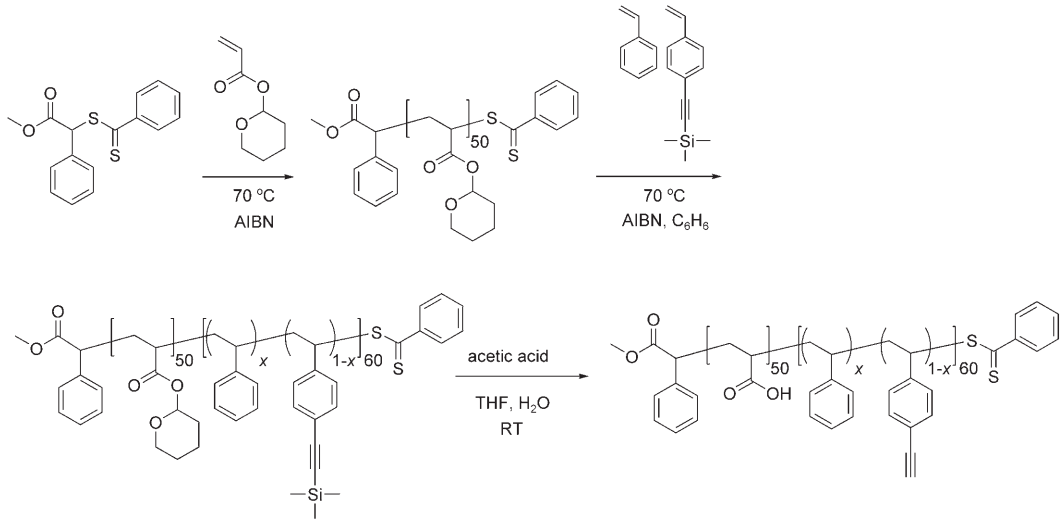

Scheme 2. Synthesis of amphiphilic diblock copolymers, PAA-*b*-[PS-*co*-PSC≡CH], **7**, having an acetylene-functionalized hydrophobic chain segment, by using sequential RAFT polymerization and copolymerization, and then acid-catalyzed hydrolysis and deprotection.

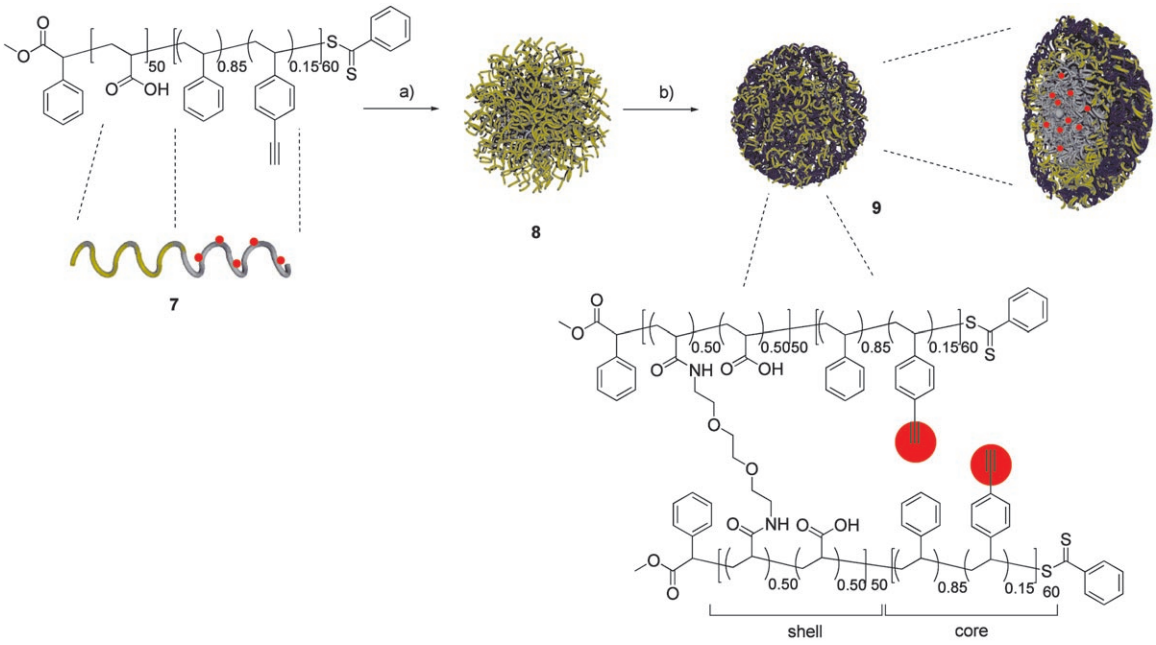

Scheme 3. Preparation of acetylene core-functionalized SCKs. a) THF, followed by addition of water and dialysis against water; b) 2,2′-(ethylenedioxy)-bis(ethylamine) (0.25 equiv based upon the acid functionalities), 1-[3′-(dimethylamino)propyl]-3-ethylcarbodiimide methiodide (0.50 equiv to acid functionalities), RT, overnight, followed by dialysis against water.

tablished chemistries, with 2,2′-(ethylenedioxy)bis(ethylamine) in the presence of 1-[3′-(dimethylamino)propyl]-3-ethylcarbodiimide methiodide.[84] The condensation reaction between the diamino cross-linkers and pendant carboxylic acid groups along the PAA segments, located in the periphery of the micelles, yielded the core-shell amphiphilic SCK nanostructures. After exhaustive dialysis against water, acetylene core-functionalized SCK nanoparticles, **9**, were isolated and characterized. The calculated concentration of the nanoparticle solution was determined by measurement of the final volume of solution obtained together with the initial weight of the polymer precursors used.

The size and shape of the micelles and SCKs (**8** and **9**, respectively) were measured on solid substrates by atomic force microscopy (AFM) and transmission electron microscopy (TEM), and in solution by using dynamic light scattering (DLS) (Table 1). Significantly, TEM analysis gave nanoparticle diameters (D_{av}) which were similar to the respective diameters obtained from DLS analysis (D_h). The low height values (H_{av}) for **8** and **9**, as measured by AFM, relative to the diameters measured by TEM indicate that significant deformation occurred upon absorption onto the hydrophilic mica surface, the substrate for AFM characterization, as opposed to the hydrophobic carbon surface, of the carbon-coated copper grid substrate for TEM analysis. Although complicated by the finite size of the AFM tip, the larger lateral sizes of the particles (D_{av}) determined by AFM analysis in comparison to those from TEM also supported greater deformation of the particles on mica. In addition, AFM particle height analysis confirmed the expected increase in rigidity upon shell cross-linking of micelle **8** to afford SCK nanoparticle **9**.

Table 1. Characterization data for micelle **8** and the corresponding SCK nanoparticle **9**.

Particle	DLS	AFM		TEM	DSC
	D_h[a] [nm]	D_{av}[b] [nm]	H_{av}[b] [nm]	D_{av}[c] (nm)	T_g[d] [°C]
8	26 ± 1	90 ± 16	0.9 ± 0.3	15 ± 1	101, 130
9	18 ± 3	81 ± 13	2.8 ± 0.3	14 ± 1	104

[a] Number-averaged hydrodynamic diameters in aqueous solution by dynamic light scattering. [b] Average heights and diameters measured by tapping-mode AFM and calculated from the values for 150 particles. [c] Average diameters measured by TEM and calculated from the values for 150 particles. [d] Glass transition temperatures, taken as the midpoint of the inflection tangent upon the third heating scan.

Differential scanning calorimetry (DSC) of micelles **8** showed two transitions (T_g), at about 130 and 100 °C, indicating domain phase separation of the PS and PAA. Upon cross-linking, the nanoparticle, **9**, displayed only one T_g, (ca. 100 °C), by DSC analysis, corresponding to the PS core, indicating the formation of a nanoparticle cross-linked in the PAA domain. IR analysis of a lyophilized sample of **9** confirmed the presence of the characteristic absorbance's for the acetylene functionality at about 3300 and 2160 cm^{-1} and also displayed new signals attributable to the ethylene glycol cross-linker at about 1100 cm^{-1}.

Click reaction within the nanoparticle core: As a result of the benign reaction conditions and structural tolerance, copper(I)-catalyzed Click chemistry has received much attention in both chemical biology and materials science.[85–88] This chemistry features complete regioselectively and fidelity in

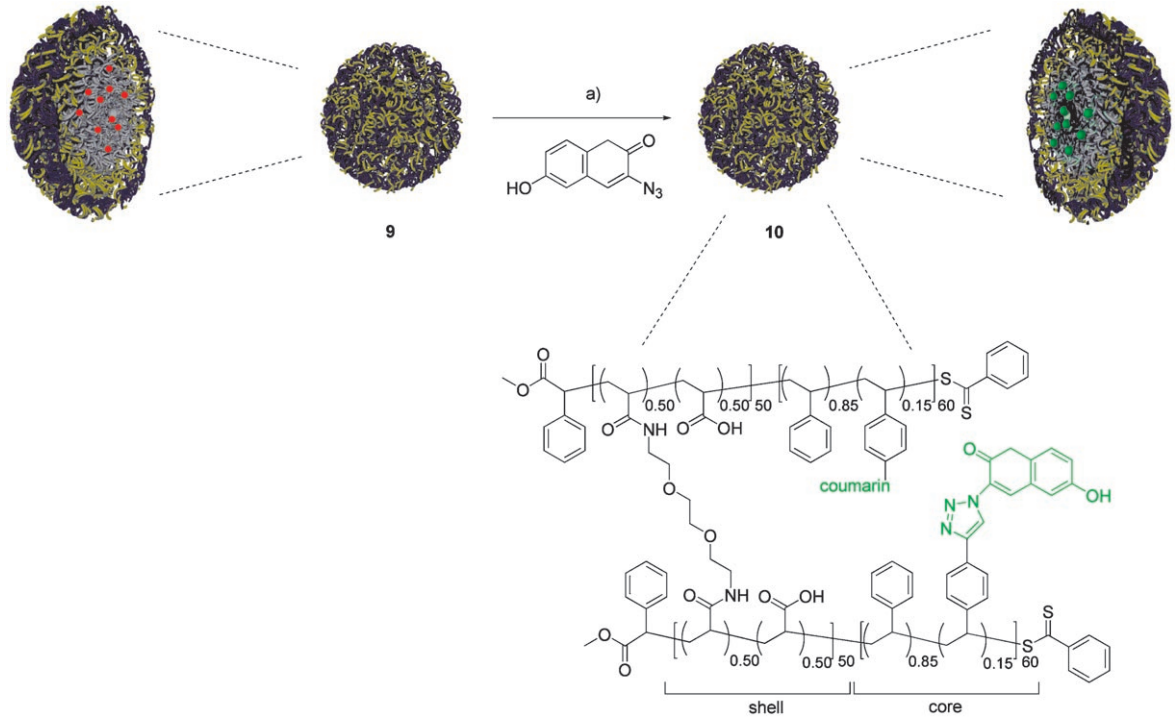

Scheme 4. Reagents and conditions: a) dialysis of **9** into THF/H_2O 4:1 for 3 d, then addition of [$CuBr(PPh_3)_3$] (0.1 equiv), and DIPEA (1.0 equiv), 3-azidocoumarin (1.11 equiv to acetylene functionality), RT, 2 d, followed by dialysis against THF/buffered H_2O 1:4 for 10 d, and then dialysis against pH 7.3 phosphate buffered saline, 4 d.

the presence of a wide range of functional groups making it a versatile and facile tool for the functionalization of surfaces and nanoparticles.[57,89] The availability of the acetylene groups within the nanoparticle core towards Click chemistry was evaluated using the fluorogenic coupling of an azido-functionalized coumarin.

The hydrophobic core of nanoparticle **9** was first swollen by dialysis for three days into a solution of 20% THF in buffered water. The Click reaction within the hydrophobic nanoparticle core was then allowed to proceed for two days at ambient temperature using an organic copper(I) catalyst, [$CuBr(PPh_3)_3$] and a reducing agent DIPEA. The reaction was then purified by exhaustive dialysis initially against a 4:1 mixture of sodium phosphate buffered saline at pH 7.3 and THF followed by dialysis against buffered H_2O to afford the fluorescent coumarin-functionalized nanoparticle **10** (Scheme 4).

DLS analysis of **10** indicated that the nanoparticles exhibited no significant increase in D_h upon functionalization with the coumarin molecule ($D_h = 19 \pm 2$ nm) while both TEM and AFM analyses showed little or no difference in particle diameter or height before and after functionalization (Figure 3).

As shown in Figure 4, 3-azidocoumarin behaved as an effective profluorophore, being fluorescently inactive when irradiated with 496 nm light, but upon cycloaddition with the acetylene functionalities within the nanoparticle core domain of **10**, formed a triazole linkage and then underwent fluorescent emission. The observed absorption maximum ($(\lambda_{max})_{ex} = 496$ nm) from UV/Vis analysis and emission maximum from fluorescence analysis ($(\lambda_{max})_{em} = 551$ nm) of nanoparticle **10**, confirms the formation of the triazole ring between the profluorophore and the nanoparticle. The control experiment using a nanoparticle without acetylene functionality was performed under identical conditions and no fluorescence was observed by UV/Vis analysis. To further confirm the formation of the triazole ring in **10**, these nanoparticles and the azido coumarin were examined under a hand-held UV lamp ($\lambda_{ex} = 365$ nm). Under these irradiation conditions, at a wavelength where both species absorb light (Figure 4a), the nanoparticles **10** were observed to fluorescence strongly whilst the azido coumarin showed non observable fluorescence.

The successful covalent attachment of the profluorophore to nanoparticle **10** was confirmed by analytical ultracentrifugation (AU) in combination with collection of the UV/Vis absorption spectra (in the range 400–600 nm) at different radial positions (top, middle and bottom of the cell) across the sedimentation equilibrium (SE) profile (Figure 5). From the data of Figure 5, it is apparent that the absorption maximum at about 500 nm at the bottom of the cell, attributable to the sedimented fluorescent nanoparticles, further confirms the covalent attachment of the dye molecule to the nanoparticles. It should be noted that the peak at 350 nm for **10** is not observed in the AU trace due to instrumentally available scan range of 400–600 nm.

The molecular weight of the nanoparticle **9** was determined by AU sedimentation equilibrium and density mea-

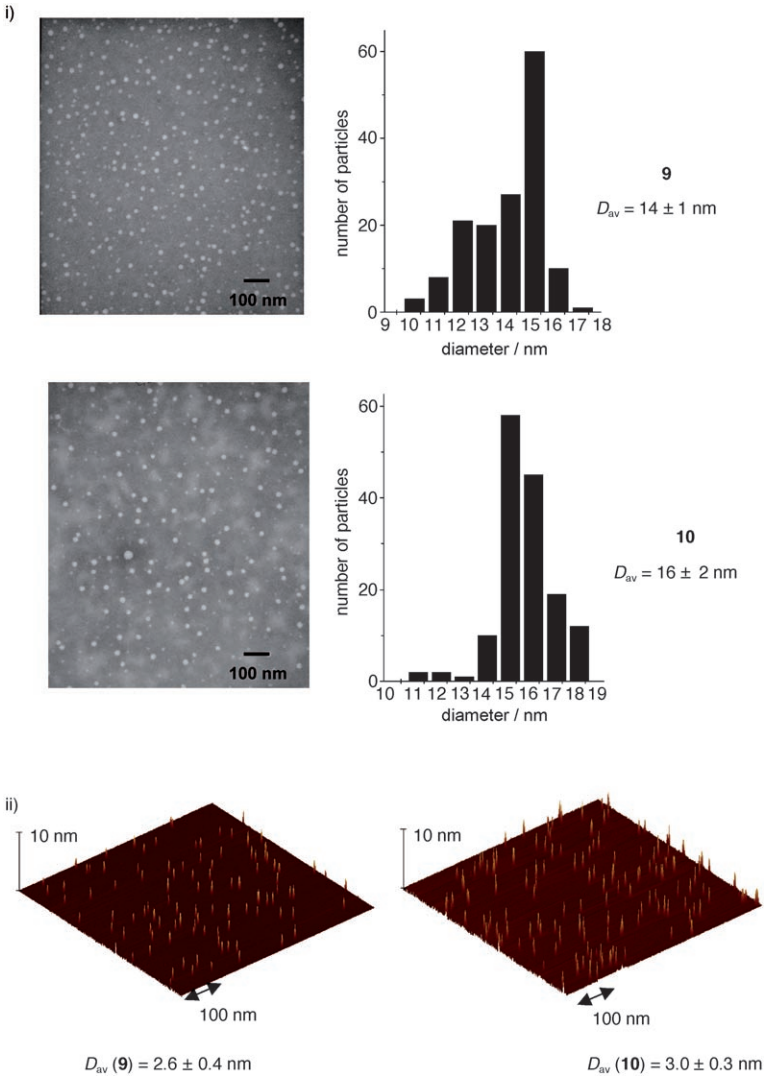

Figure 3. i) TEM images of nanoparticles **9** and **10**. Average diameters are shown with the corresponding distribution and a representative image. Samples were stained with phosphotungstic acid and drop deposited onto a carbon-coated copper grid; ii) representative tapping-mode AFM images of nanoparticles **9** and **10**. Samples were prepared by drop deposition onto freshly cleaved mica and allowed to dry under ambient conditions.

surements to be $260\,000 \pm 185\,000\ g\,mol^{-1}$, and the aggregation number was calculated to be 22 ± 17 chains/particle. The molecular weight and aggregation number are not available for the micelle, **8**, since the supramolecularly assembled nanostructures are under constant reorganization and concentrating the sample for analysis would alter the size of the micelle. The molecular weight and aggregation number data for **10** were not determined, as the particle had not been altered in a way that would significantly affect the values, relative to those measured for **9**.

Conclusion

The synthesis of a novel class of block copolymers incorporating acetylene functionality in the hydrophobic block has been accomplished using RAFT polymerization techniques. The conversion of these polymers into amphiphilic block copolymers requires careful consideration in the choice of compatible protecting group chemistry for both the acetylene and poly(acrylic) acid functionalities. In this study, tetrahydropyran acrylate was successfully utilized and ester deprotection under mild acidic conditions also allowed simultaneous removal of the TMS acetylene protecting group. This single-step deprotection strategy afforded amphiphilic block copolymers with the acetylene functionality intact and available for Click reactions. These amphiphilic block copolymers were successfully self-assembled into micelles and SCK nanoparticles with the specific incorporation of the acetylene functional groups within the core domain, enabling highly efficient and compatible Click chemistry to be performed within the hydrophobic core of the nanoparticles. In this fundamental study, the successful covalent attachment of a fluorogenic probe within the nanoparticle core was confirmed by fluorescence spectroscopy and analytical ultracentrifugation. The importance of advances made through the work reported here, involving balancing of polymerization chemistry, supramolecular assembly and covalent stabilization to produce well-defined nanostructures having accessible, reactive functionalities localized within the core domain, will continue to be realized as further developments are pursued toward transformation of these SCKs into sophisticated nanoscopic containment vessels.

Experimental Section

Instrumentation: NMR (^{1}H and ^{13}C) spectra were collected on a Bruker AVANCE 400 FT-NMR spectrometer using deuterated solvents. Coupling constants are reported in Hertz, and chemical shifts are reported in parts per million (δ) relative to $CHCl_3$ (7.26 ppm for ^{1}H and 77.2 ppm for ^{13}C) or DMSO (2.50 ppm for ^{1}H and 39.52 ppm for ^{13}C) as internal reference. Gel permeation chromatography was performed in THF on a Waters chromatograph equipped with four 5 μm Waters columns (300 × 7.7 mm) connected in series with increasing pore size (100, 1000, 10000,

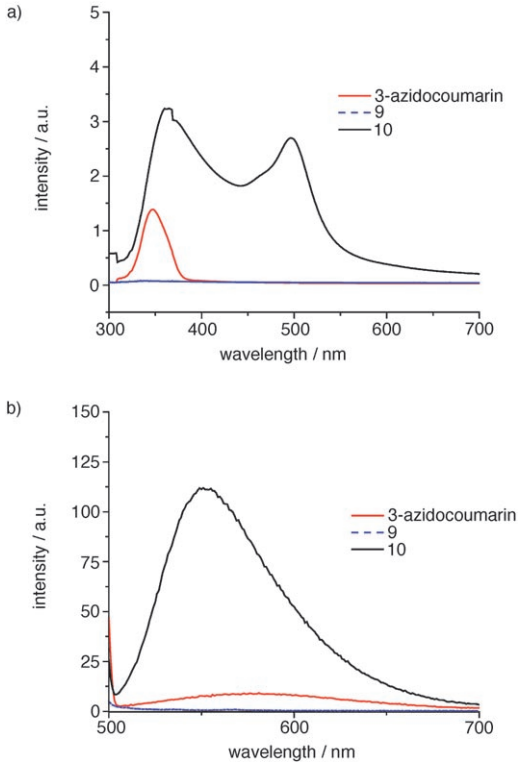

Figure 4. a) Comparison of UV/Vis absorption spectra for **9**, **10** and 3-azidocoumarin all at ca. 0.2 mg mL^{-1}; b) comparison of fluorescence emission spectra (excitation wavelength $\lambda_{ex}=496$ nm) for **9**, **10** and 3-azidocoumarin.

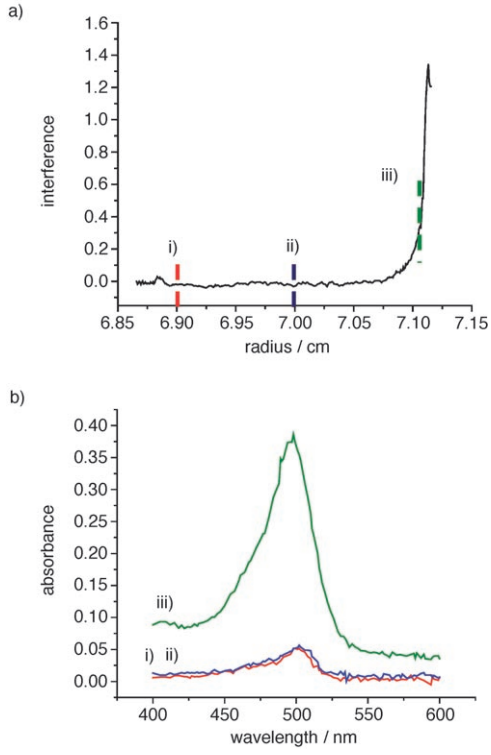

Figure 5. a) Sedimentation equilibrium profile (5000 rpm) collected using an interferometry detector for the nanoparticle **10** and b) corresponding absorption spectra, recorded at different radial positions, i) top, ii) middle, and iii) bottom, across the sedimentation equilibrium profile.

1 000 000 Å). Waters 410 differential refractometer index (DRI) and 996 photodiode array detectors were employed. The molecular weights of the polymers were calculated relative to linear polystyrene standards. The modulated differential scanning calorimetry (DSC) measurements were performed with a TA Instruments, DSC 2920 and with a ramp rate of 4° per minute. The glass-transition temperatures (T_g) were taken as the midpoint of the inflection tangent, upon the third heating scan. IR spectra were obtained on Perkin-Elmer Spectrum BX FT-IR system using drop deposition onto NaCl plates. UV/Vis spectroscopy data were acquired on a Varian Cary 1E UV/Vis spectrophotometer. Fluorescence spectroscopy data were acquired on a Varian Cary Eclipse Fluorescence spectrophotometer, each sample was excited at $\lambda_{ex}=496$ nm, and the fluorescence emission spectra in the range 500–700 nm were recorded.

Hydrodynamic diameters (D_h) and size distributions for the SCKs in aqueous solutions were determined by dynamic light scattering (DLS). The DLS instrumentation consisted of a Brookhaven Instruments Limited (Worcestershire, U.K.) system, including a model BI-200SM goniometer, a model BI-9000 AT digital correlator, a model EMI-9865 photomultiplier, and a model 95-2 Ar ion laser (Corp. Lexel, Farmindale, NY) operated at 514.5 nm. Measurements were made at 20 ± 1 °C. Prior to analysis, solutions were centrifuged in a model 5414 microfuge (Inc. Brinkman Instruments, Westbury, NY) for 4 min to remove dust particles. Scattered light was collected at a fixed angle of 90 °C. The digital correlator was operated with 522 ratio spaced channels, and initial delay of 0.1 μs, a final delay of 5.0 μs, and a duration of 15 min. A photomulitplier aperture of 200 μm was used, and the incident laser intensity was adjusted to obtain a photon counting of between, 200 and 300 kcps. Only measurements in which the measured and calculated baselines of the intensity autocorrelation function agreed to within 0.1 % were used to calculate particle size. The calculations of the particle size distributions and distribution averages were performed with the ISDA software package (Brookhaven Instruments Company), which employed single-exponential fitting, cumulants analysis, non-negatively constrained least-squares (NNLS) or CONTIN particle size distribution analysis routines. All determinations were made in triplicate.

The height measurements and distributions for the nanoparticles were determined by tapping-mode AFM under ambient conditions in air. The AFM instrumentation consisted of a Nanoscope III BioScope system (Digital Instruments, Veeco Metrology Group; Santa Barbara, CA) and standard silicon tips (type, OTESPA-70; L, 160 μm; normal spring constant, 50 N m^{-1}; resonance frequency, 246–282 kHz). The sample solutions were prepared for AFM analysis by dilution (typical concentrations between 0.02–0.0002 mg mL^{-1}) and deposition of a drop (2 μL) onto freshly cleaved mica and allowed to dry freely in air. The number-average particle heights (H_{av}) and diameter (D_{av}) values and standard deviations were generated from the sectional analysis of 150 particles from at least five different analysis regions.

Transmission electron microscopy samples were diluted in water (9:1) and further diluted with a 1 % phosphotungstic acid (PTA) stain (1:1). Carbon grids were prepared by oxygen plasma treatment to increase the surface hydrophilicity. Micrographs were collected at 100 000 × magnification and calibrated using a 41 nm polyacrylamide bead from NIST. Histograms of number average particle diameters (D_{av}) and standard deviations were generated from the analysis of a minimum of 150 particles from at least three different micrographs.

Sedimentation equilibrium experiments were conducted on a Beckman Instruments, Inc. (Fullerton, CA) model Optima XL-I analytical ultracentrifuge fitted with a model An60-Ti four-hole rotor, and Epon charcoal-filled, six-channel centerpiece sample cells with matched quartz windows. Data were recorded using the instrument's Rayleigh interfometric (refractive index) detection optics at 20 °C 3000, 4000, and 5000 rpm, with a centrifugation time of 3–5 d to reach sedimentation equilibrium. The solution volume was 110 μL, and the optical path length was 12 mm. A Mettler–Parr model DMA 602 high-precision digital density meter was employed to determine the density at 20.0 °C for all solutions. All densities were an average of five runs, with measurements of one hundred periods per run. The molecular weight and weight-average degree of aggregation, N_{agg}, was computed as previously reported.[90] Interference scans

were obtained after sedimentation equilibrium had been reached, and then using this profile various radial positions in the cell (designated top, middle and bottom) were identified and scanned using the UV/Vis detection optics.

Materials and methods: *tert*-Butyl acrylate (*t*BuA) and styrene (S) were purified by vacuum distillation from CaH_2 and then stored at −15 °C. AIBN was recrystallized twice from diethyl ether. Tetrahydrofuran (THF) was dried by prolonged heating at reflux over sodium/benzophenone. All other materials were used as received from Sigma-Aldrich Company. Supor 25 mm, 0.1 μm Spectra/Por membrane tubes (molecular weight cut-off (MWCO) 3.5 or 6–8 kDa, Spectrum Medical Industries, Inc., Laguna Hills, CA) were used for dialysis. Stirred ultrafiltration cell and ultrafiltration membrane filter discs (NMWL 10 kDa, Millipore Corporation, Bedford, MA) were used for concentration and dialysis of nanoparticle solutions. The following materials were synthesized according to literature methods; 4-(trimethylsilylethynyl)styrene,[91] tetrahydropyran acrylate,[79] 2,2,5-trimethyl-3-(phenylethoxy)-4-phenyl-3-azahexane,[83] 2,2,5-trimethyl-4-phenyl-3-azahexane-3-nitroxide,[83] (*S*)-methoxycarbonylphenylmethyl dithiobenzoate,[80] 3-azidocoumarin,[61] [CuBr-$(PPh_3)_3$].[92]

P*t*BuA homopolymer (1): A mixture of the alkoxyamine (2,2,5-trimethyl-3-(1-phenylethoxy)-4-phenyl-3-azahexane) (194 mg, 0.6 mmol), the corresponding nitroxide (2,2,5-trimethyl-4-phenyl-3-azahexane-3-nitroxide) (6.6 mg, 0.03 mmol), and *tert*-butyl acrylate (15.0 g, 118 mmol), were degassed by three freeze/pump/thaw cycles, sealed under argon, and heated at 125 °C for 26 h. The viscous reaction mixture was then dissolved in THF (20 mL) and precipitated three times into 10 % H_2O in MeOH (600 mL) at 4 °C. The tacky precipitate was then dissolved in THF (100 mL) and dried over $MgSO_4$ for 2 h. The solution was filtered and the filtrate was reduced to dryness by rotary evaporation. The resulting white solid **1** was dried under vacuum overnight (7.65 g, 51 %). M_n^{NMR} = 13400 g mol^{-1}, M_n^{GPC} = 13000 g mol^{-1}, M_w/M_n = 1.17; DSC: (T_g) = 51 °C; IR: $\tilde{\nu}$ = 3058–2868, 1731, 1480, 1455, 1393, 1368, 1259, 1151, 1071, 1032, 910, 846, 752, 699 cm^{-1}; ^{1}H NMR ($CDCl_3$): δ = 7.19–7.10 (m, Ar-*H* from initiator), 2.22–2.06 (br, C*H* of the polymer backbone), 1.81–1.25 (br, *meso* and racmo CH_2 of the polymer backbone), 1.51–1.21 (br, $(CH_3)_3$C); ^{13}C NMR ($CDCl_3$): δ = 174.5–174.3 (*C*(O)), 80.8–80.7 (*C*$(CH_3)_3$), 42.7–42.2 (α carbon of the polymer backbone), 37.3–35.4 (β carbon of the polymer backbone), 28.4 (C(*C*H_3)$_3$).

P*t*BuA$_{100}$-*b*-[PS-*co*-PSC≡CTMS]$_{150}$ diblock copolymer (2): Poly(*t*BuA) macroinitiator (M_n^{GPC} = 13000 g mol^{-1}, M_w/M_n = 1.17; 5.0 g, 0.39 mmol), **1**, was re-dissolved in styrene (6.0 g, 57 mmol) and 4-(trimethylsilylethynyl)-styrene (2.33 g, 11.4 mmol) and the solution was degassed by three freeze/pump/thaw cycles, sealed under argon, and heated at 125 °C for 12 h. The solidified reaction mixture was then re-dissolved in THF (20 mL) and precipitated into cold MeOH (2 × 800 mL). The precipitate was collected by vacuum filtration and dried overnight in vacuo, to give the desired block copolymer **2** as a white solid (9.20 g, 55 %). M_n^{NMR} = 32300 g mol^{-1}, M_n^{GPC} = 32000 g mol^{-1}, M_w/M_n = 1.24; DSC: $(T_g)_{PtBuA}$ = 50 °C, $(T_g)_{PS\text{-}co\text{-}PSC\equiv CTMS}$ = 96 °C; IR: $\tilde{\nu}$ = 3100–2850, 2157, 1729, 1601, 1493, 1452, 1392, 1367, 1260, 1150, 1029, 865, 845, 759, 669 cm^{-1}; ^{1}H NMR ($CDCl_3$): δ = 7.34–6.14 (m, 9 Ar-*H*), 2.24–2.05 (br, C*H* of the polymer backbone), 1.99–1.08 (CH_2 of the polymer backbone), 1.22–1.14 (s, $(CH_3)_3$C), 0.23–0.17 (s, C≡CSi$(CH_3)_3$); ^{13}C NMR ($CDCl_3$): δ = 174.9–174.3 (*C*(O)), 145.9–145.0 (2 Ar-*C*), 134.6–132.2 (8 Ar-*C*), 128.7-126.1 (2 Ar-*C*), 106.3–104.6 (*C*≡CSi$(CH_3)_3$), 93.4–92.9 (C≡*C*Si$(CH_3)_3$), 80.8–80.7 (*C*$(CH_3)_3$), 42.8–35.7 (*C*H and CH_2 of polymer backbone), 28.5–28.4 (C-(*C*H_3)$_3$, 0.5–0.4 (C≡CSi(*C*H_3)$_3$).

P*t*BuA$_{100}$-*b*-[PS-*co*-PSC≡CH]$_{150}$ diblock copolymer (3): P*t*BuA$_{100}$-*b*-[PS-*co*-PSC≡CTMS]$_{150}$ (M_n^{GPC} = 32000 g mol^{-1}, M_w/M_n = 1.24; 1.80 g, 1.24 mmol of TMS) was added to a 100 mL, round-bottom flask equipped with a stirrer bar, followed by dry tetrahydrofuran (60 mL). The mixture was allowed to stir for 30 min to dissolve the polymer and then cooled to 0 °C. Tetrabutylammonium fluoride (1.0 M solution in tetrahydrofuran) (TBAF; 6.9 mL, 6.2 mmol, 5.0 equiv to the TMS group) was then added, at 0 °C. After the mixture was allowed to stir overnight at RT, the tetrahydrofuran and excess TBAF were removed in vacuo. The resultant solid was re-dissolved in THF (15 mL) and precipitated into cold MeOH (2 × 600 mL). The powdery off white solid was vacuum dried to afford P*t*BuA$_{100}$-*b*-[PS-*co*-PSC≡CH]$_{150}$, **3** (1.64 g, 96 %). M_n^{NMR} = 31600 g mol^{-1}, M_n^{GPC} = 30900 g mol^{-1}, M_w/M_n = 1.25; DSC: $(T_g)_{PtBuA}$ = 51 °C, $(T_g)_{PS\text{-}co\text{-}PSC\equiv CH}$ = 97 °C; IR: $\tilde{\nu}$ = 3290, 3060–2875, 2158, 1728, 1605, 1493, 1452, 1392, 1251, 1151, 1070, 906, 845, 760, 670 cm^{-1}; ^{1}H NMR ($CDCl_3$): δ = 7.36–6.11 (m, 9 Ar-*H*), 3.01–2.90 (C≡C*H*), 2.21–2.01 (br, C*H* of the polymer backbone), 1.95–1.12 (CH_2 of the polymer backbone), 1.21–1.13 (s, $(CH_3)_3$C); ^{13}C NMR ($CDCl_3$): δ = 175.0–174.1 (*C*(O)), 146.2–145.3 (2 Ar-*C*), 134.8–133.5 (8 Ar-*C*), 128.5-126.2 (2 Ar-*C*), 84.2–83.4 (*C*≡CH), 80.8–80.6 (*C*$(CH_3)_3$), 77.7–76.9 (C≡*C*H), 42.7–40.6 (*C*H and CH_2 of polymer backbone), 38.2–35.9 (*C*H and CH_2 of polymer backbone), 28.6–28.4 (C-(*C*H_3)$_3$).

PTHPA using NMP, 4: A mixture of the alkoxyamine (2,2,5-trimethyl-3-(1-phenylethoxy)-4-phenyl-3-azahexane) (194 mg, 0.6 mmol), the corresponding nitroxide (2,2,5-trimethyl-4-phenyl-3-azahexane-3-nitroxide) (6.6 mg, 0.03 mmol), and tetrahydropyran acrylate (14.0 g, 89.7 mmol), were degassed by three freeze/pump/thaw cycles, sealed under argon, and heated at 100 °C for 16 h. The viscous reaction mixture was then dissolved in THF (20 mL) and precipitated three times into hexane (400 mL) at ca. −70 °C. The resulting white solid was dried under vacuum overnight, to afford **4** (4.42 g, 32 %), M_n^{NMR} = 5900 g mol^{-1}, M_n^{GPC} = 5200 g mol^{-1}, M_w/M_n = 1.50; DSC: $(T_g)_{PTHPA}$ = 49 °C, $(T_g)_{PAA}$ = 131 °C; IR: $\tilde{\nu}$ = 3540–2960, 2864, 1732, 1706, 1454, 1346, 1266, 1172, 1074, 1017, 910, 898, 861, 805 cm^{-1}; ^{1}H NMR ($CDCl_3$): δ = 12.74–12.36 (COO*H*), 7.24–7.11 (m, Ar-*H* from initiator), 6.02–5.85 (C(O)OC*H*CH$_2$), 3.91–3.72 (C(O)OCHCH_2), 3.70–3.52 (C(O)OCHCH_2), 2.42–2.06 (br, C*H* of the polymer backbone), 1.91–1.17 (br, *meso* and racmo CH_2 of the polymer backbone and CH_2 of THP group), 1.51–1.10 (br, CH_2CH_2 of THP group); ^{13}C NMR ($CDCl_3$): δ = 176.3–175.6 (*C*OOH), 174.5–174.3 (*C*OOTHP), 101.3–101.0 (C(O)O*C*HCH$_2$), 63.7–63.1 (*C*H$_2$ of THP group), 42.6–35.2 (α and β carbons of the polymer backbone), 32.0–27.8 (2*C*H$_2$ of THP), 19.7–18.3 (*C*H$_2$ of THP).

PTHPA using RAFT, 5: A mixture of (*S*)-methoxycarbonylphenylmethyl dithiobenzoate (72 mg, 0.24 mmol), AIBN (4.0 mg, 0.02 mmol), and tetrahydropyran acrylate (5.6 g, 36 mmol), were degassed by three freeze/pump/thaw cycles, sealed under argon, and heated at 70 °C for 22 h. The viscous reaction mixture was then dissolved in THF (10 mL) and precipitated three times into hexane (200 mL) at ca. −70 °C. The resulting pale pink solid, **5** was dried under vacuum overnight (2.2 g, 39 %). M_n^{NMR} = 8400 g mol^{-1}, M_n^{GPC} = 8300 g mol^{-1}, M_w/M_n = 1.18; DSC: $(T_g)_{PTHPA}$ = 48 °C; IR: $\tilde{\nu}$ = 3021–2773, 1739, 1444, 1355, 1251, 1207, 1161, 1117, 1036, 1023, 941, 899, 866, 820 cm^{-1}; ^{1}H NMR ($CDCl_3$): δ = 5.99–5.87 (C(O)OC*H*CH$_2$), 3.93–3.75 (C(O)OCHCH_2), 3.71–3.59 (C(O)OCHCH_2), 2.51–2.10 (br, C*H* of the polymer backbone), 2.08–1.17 (br, *meso* and racmo CH_2 of the polymer backbone and 3CH_2 of THP group); ^{13}C NMR ($CDCl_3$): δ = 174.2–174.5 (*C*OOTHP), 102.0–101.4 (C(O)O*C*HCH$_2$), 63.3–62.9 (*C*H$_2$ of THP group), 43.8–37.6 (α and β carbons of the polymer backbone), 32.2–28.1 (2*C*H$_2$ of THP), 20.2–19.5 (*C*H$_2$ of THP).

PTHPA$_{50}$-*b*-[PS-*co*-PSC≡CTMS]$_{60}$ diblock copolymer using RAFT, 6: PTHPA macroinitiator (M_n^{GPC} = 8300 g mol^{-1}, M_w/M_n = 1.18; 1.5 g, 0.18 mmol), **5**, was re-dissolved in styrene (3.0 g, 29 mmol), 4-trimethylethenylstyrene (0.38 g, 1.9 mmol), benzene (1.5 mL), and AIBN (1.6 mg, 0.26 mmol) were added. The solution was degassed by three freeze/pump/thaw cycles, sealed under argon, and heated at 70 °C for 10 h. The solidified reaction mixture was then re-dissolved in THF (20 mL) and precipitated into cold hexane (2 × 800 mL). The precipitate was collected by vacuum filtration and dried overnight in vacuo, to give the desired block copolymer, **6**, as a pale pink solid (2.20 g, 54 %). M_n^{NMR} = 15100 g mol^{-1}, M_n^{GPC} = 16200 g mol^{-1}, M_w/M_n = 1.15; DSC: $(T_g)_{PTHPA}$ = 47 °C, $(T_g)_{PS\text{-}co\text{-}PSC\equiv CTMS}$ = 93 °C; IR: $\tilde{\nu}$ = 3060–2830, 2157, 1738, 1601, 1543, 1493, 1259, 1179, 1070, 1028, 965, 906, 804, 758, 699 cm^{-1}; ^{1}H NMR ($CDCl_3$): δ = 7.26–6.28 (m, 9 Ar-*H*), 6.02–5.89 (C(O)OC*H*CH$_2$), 3.95–3.71 (C(O)OCHCH_2), 3.68–3.55 (C(O)OCHCH_2), 2.50–2.18 (br, C*H* of the polymer backbone), 2.08–1.15 (br, *meso* and racmo CH_2 of the polymer backbone and 3CH_2 of THP group), 0.22–0.18 (C≡CSi$(CH_3)_3$); ^{13}C NMR ($CDCl_3$): δ = 173.9–172.7 (*C*OOTHP), 154.2–149.7 (2 Ar-*C*), 139.3–137.5 (8 Ar-*C*), 139.3-129.5 (2 Ar-*C*), 104.8–104.1 (*C*≡CSi$(CH_3)_3$),

103.3–102.8 (C(O)O*C*HCH$_2$), 101.6–99.3 (C≡*C*Si(CH$_3$)$_3$), 64.2–63.1 (*C*H$_2$ of THP group), 44.0–37.4 (α and β carbons of the polymer backbone), 32.1–27.9 (2*C*H$_2$ of THP), 21.4–19.7 (*C*H$_2$ of THP), 0.5–0.4 (C≡CSi-(*C*H$_3$)$_3$).

PAA$_{50}$-*b*-[PS-co-PSC≡CH]$_{60}$ diblock copolymer, 7: PTHPA$_{50}$-*b*-[PS-*co*-PSC≡CTMS]$_{60}$ (M_n^{GPC} = 16200 g mol^{-1}, M_w/M_n = 1.15; 1.0 g, 3.31 mmol of ester groups and 0.74 mmol of TMS groups) was added to a 100 mL, round-bottom flask equipped with a stirrer bar, followed by tetrahydrofuran (20 mL). The mixture was allowed to stir for 30 min to dissolve the polymer and then deionized water was added (10.0 mL), followed by glacial acetic acid (40 mL). After the mixture was allowed to stir overnight at RT, the polymer was further purified by transfer to presoaked dialysis membrane tubes (MWCO ca. 6–8 kDa), and dialysis against deionized water for 4 d. Lyophilization gave **7** as a pale pink solid, (0.68 g, 95 %). DSC: $(T_g)_{PAA}$ = 131 °C, $(T_g)_{PS\text{-}co\text{-}PSC\equiv CH}$ = 96 °C; IR: $\tilde{\nu}$ = 3550–2830, 3310, 3020–2860, 2157, 1710, 1493, 1452, 1396, 1249, 1163, 1065, 1024, 864, 841, 759, 699, 669 cm^{-1}; ^{1}H NMR ([D$_6$]DMSO): δ = 13.2–11.9 (br, COO*H*), 7.4–6.1 (m, 9 Ar-*H*), 3.1–3.0 (C≡C*H*), 2.3–1.0 (br, C*H* and C*H*$_2$ of polymer backbone); ^{13}C NMR ([D$_6$]DMSO): δ 176.1–175.6 (*C*OOH), 151.2–148.3 (2 Ar-*C*), 137.8–135.5 (8 Ar-*C*), 134.5-128.3 (2 Ar-*C*), 85.6–83.0 (*C*≡CH), 79.2–78.5 (C≡*C*H), 45.9–37.4 (*C*H and *C*H$_2$ of polymer backbone).

PAA$_{50}$-*b*-[PS-*co*-PSC≡CH]$_{60}$ micelle, 8: A round-bottom flask equipped with a stirrer bar was charged with PAA$_{50}$-*b*-[PS-*co*-PSC≡CH]$_{60}$, **7**, (M_n^{NMR} = 10800 g mol^{-1}; 0.50 g, 2.31 mmol of acrylic acid groups), THF (500 mL) was added and the solution was allowed to stir at RT for 30 min to ensure the mixture was homogenous. Deionized water (500 mL) was added via a metering pump at the rate of 20 mL h^{-1}. After all of the water had been added, the bluish micelle solution was transferred to dialysis tubing (MWCO ca. 6–8 kDa), and dialyzed against deionized water for 4 d, to remove all of the THF. The final volume of **8** was 1.6 L, affording a polymer concentration of ca. 0.30 mg mL^{-1}. D_h (DLS) = 26 ± 1 nm; D_{av} (TEM): 15 ± 1 nm; D_{av} (AFM): 90 ± 16 nm; H_{av} (AFM): 0.9 ± 0.3 nm. Lyophilization gave **8** as a pale pink solid. DSC: $(T_g)_{PAA}$ = 130 °C, $(T_g)_{PS}$ = 101 °C.

Acetylene-functionalized SCK nanoparticle, 9: A solution of 2,2′-(ethylenedioxy)*bis*(ethylamine) (0.026 g, 0.17 mmol) in deionized water (5.0 mL) was added to a stirred solution of micelle **8** (500 mL, 0.30 mg mL^{-1}, 0.69 mmol of acrylic acid, 0.14 mmol of acetylene groups) in a round-bottom flask equipped with a stirrer bar, dropwise over 10 min. The solution was allowed to stir for 1 h at RT. To this reaction mixture was added dropwise, via a metering pump at the rate of 15 mL h^{-1}, a solution of 1-[3′-(dimethylamino)propyl]-3-ethylcarbodiimide methiodide (0.10 g, 0.35 mmol) dissolved in deionized water (100 mL). The reaction mixture was allowed to stir overnight at RT and was then transferred to presoaked dialysis membrane tubes (MWCO ca. 6–8 kDa), and dialyzed against deionized water for 4 d to remove small molecule contaminants. Final concentration of solution of **9** ca. 0.23 mg mL^{-1}. D_h (DLS) = 18 ± 3 nm; D_{av} (TEM): 14 ± 1 nm; D_{av} (AFM): 81 ± 13 nm; H_{av} (AFM): 2.6 ± 0.4 nm. Lyophilization gave **9** as a pale pink solid. DSC: $(T_g)_{PS}$ = 104 °C. IR: $\tilde{\nu}$ = 3319, 3027–2852, 2153, 1716, 1704, 1657, 1638, 1565, 1442, 1248, 1197, 1102, 1053, 780, 702 cm^{-1}.

Reaction of core acetylene-functionalized nanoparticle with 3-azidocoumarin, 10: A solution of nanoparticle **9** (300 mL, 0.23 mg mL^{-1}, 0.063 mmol of acetylene groups) was transferred to presoaked dialysis membrane tubes (MWCO ca. 6–8 kDa), and dialyzed against a 1:4 THF and buffered H$_2$O mixture (50 mM sodium phosphate, 1.0 M sodium chloride, pH 7.3) for 3 d. This afforded a nanoparticle solution of concentration ca. 0.40 mg mL^{-1}. A 50 mL round-bottom flask was charged with a magnetic stir bar, 3-azidocoumarin (0.009 g, 0.046 mmol), [CuBr(PPh$_3$)$_3$] (0.0039 g, 0.004 mmol), *N*,*N*′-diisopropylethylamine (DIPEA) (0.0054 g, 0.042 mmol), THF (2 mL), and H$_2$O (8 mL). The mixture was allowed to stir at RT for 30 min and was then added to a 250 mL round-bottom flask that was charged with **9** (125 mL, 0.042 mmol of acetylene groups in THF/H$_2$O). The reaction mixture was allowed to stir for 2 d at RT and transferred to presoaked dialysis membrane tubes (MWCO ca. 6–8 kDa), and dialyzed against a 4:1 mixture of buffered H$_2$O (50 mM sodium phosphate, 1.0 M sodium chloride, pH 7.3) and THF for 10 d to remove excess 3-azidocoumarin and copper catalyst. After this time, the solution was then dialyzed into buffered water (50 mM sodium phosphate, 1.0 M sodium chloride, pH 7.3) for 4 d. D_h (DLS) = 19 ± 2 nm; D_{av} (TEM): 16 ± 2 nm; D_{av} (AFM): 78 ± 14 nm; H_{av} (AFM): 3.0 ± 0.3 nm. Lyophilization gave **10** as an off-white solid. DSC: $(T_g)_{PS}$ = 103 °C; IR: $\tilde{\nu}$ = 3308, 3100–2860, 1714, 1701, 1683, 1622, 1636, 1455, 1344, 1319, 1260, 1226, 1155, 1127, 1062, 841, 759, 699 cm^{-1}.

Acknowledgements

These results are based upon work supported by the National Science Foundation under Grant number 0451490, CHE-0514031, and the Nanoscale Interdisciplinary Research Team (NIRT) program Grant number 0210247. R.K.O'R. was partially supported by a Research Fellowship from the Royal Commission for the Exhibition of 1851. M.J.J. was supported by a Chemistry-Biology Interface Program Fellowship under an NIH Training Grant No. NIH NRSA 5-T32-GM08785-0. Mr. Wenhao Lui is thanked for synthesis of the RAFT agents and preliminary polymerization results. Mr. G. Michael Veith, of the Washington University Department of Biology, is gratefully acknowledged for TEM analysis. Ms. Lucy Li (IBM) and Mr. Teddie Magbitang (IBM) are thanked for assistance with thermal and GPC analysis respectively. Mr. Jeffery L. Turner is thanked for schematic drawings of micelle and SCK nanoparticles. Prof. Qing Wang is thanked for valuable conversations and guidance (University of South Carolina).

[1] K. Kataoka, A. Harada, Y. Nagasaki, *Adv. Drug Delivery Rev.* **2001**, *47*, 113.
[2] Y. Kakizawa, K. Kataoka, *Adv. Drug Delivery Rev.* **2002**, *54*, 203.
[3] R. Langer, *Science* **2001**, *293*, 58.
[4] K. L. Wooley, *J. Polym. Sci. Polym. Chem.* **2000**, *38*, 1397.
[5] A. Rosler, G. W. M. Vandermeulen, H. A. Klok, *Adv. Drug Delivery Rev.* **2001**, *53*, 95.
[6] D. M. Lynn, M. M. Amiji, R. Langer, *Angew. Chem.* **2001**, *113*, 1757; *Angew. Chem. Int. Ed.* **2001**, *40*, 1707.
[7] M. A. Moses, H. Brem, R. Langer, *Cancer Cell* **2003**, *4*, 337.
[8] D. M. Vriezema, M. C. Aragones, J. A. A. W. Elemans, J. J. L. M. Cornelissen, A. E. Rowan, R. J. M. Nolte, *Chem. Rev.* **2005**, *105*, 1445.
[9] E. R. Gillies, J. M. J. Fréchet, *Chem. Commun.* **2003**, 1640.
[10] G. S. Kwon, T. Okano, *Adv. Drug Delivery Rev.* **1996**, 21, 107.
[11] C. Allen, A. Maysinger, A. Eisenberg, *Colloids Surf. B* **1999**, *16*, 3.
[12] F. J. M. Hoeben, P. Jonkheijm, E. W. Meijer, A. P. H. J. Schenning, *Chem. Rev.* **2005**, *105*, 1491.
[13] T. P. Lodge, *Macromol. Chem. Phys.* **2003**, *204*, 265.
[14] K. L. Wooley, *Chem. Eur. J.* **1997**, *3*, 1397.
[15] O. Terreau, L. B. Luo, A. Eisenberg, *Langmuir* **2003**, *19*, 5601.
[16] A. Choucair, C. Lavigueur, A. Eisenberg, *Langmuir* **2004**, *20*, 3894.
[17] S. E. Webber, *J. Phys. Chem. B* **1998**, *102*, 2618.
[18] D. E. Discher, A. Eisenberg, *Science* **2002**, *297*, 967.
[19] C. J. Hawker, A. W. Bosman, E. Harth, *Chem. Rev.* **2001**, *101*, 3661.
[20] M. Kamigaito, T. Ando, M. Sawamoto, *Chem. Rev.* **2001**, *101*, 3689.
[21] K. Matyjaszewski, J. H. Xia, *Chem. Rev.* **2001**, *101*, 2921.
[22] J. Chiefari, Y. K. Chong, F. Ercole, J. Krstina, J. Jeffery, T. P. T. Le, R. T. A. Mayadunne, G. F. Meijs, C. L. Moad, G. Moad, E. Rizzardo, S. H. Thang, *Macromolecules* **1998**, *31*, 5559.
[23] Y. K. Chong, T. P. T. Le, G. Moad, E. Rizzardo, S. H. Thang, *Macromolecules* **1999**, *32*, 2071.
[24] R. T. A. Mayadunne, E. Rizzardo, J. Chiefari, Y. K. Chong, G. Moad, S. H. Thang, *Macromolecules* **1999**, *32*, 6977.
[25] J. F. Quinn, R. P. Chaplin, T. P. Davis, *J. Polym. Sci. Polym. Chem.* **2002**, *40*, 2956.
[26] C. M. Schilli, M. F. Zhang, E. Rizzardo, S. H. Thang, Y. K. Chong, K. Edwards, G. Karlsson, A. H. E. Muller, *Macromolecules* **2004**, *37*, 7861.
[27] M. Stenzel-Rosenbaum, T. P. Davis, V. Chen, A. G. Fane, *J. Polym. Sci. Polym. Chem.* **2001**, *39*, 2777.

[28] R. T. A. Mayadunne, E. Rizzardo, J. Chiefari, J. Krstina, G. Moad, A. Postma, S. H. Thang, *Macromolecules* **2000**, *33*, 243.
[29] M. Benaglia, E. Rizzardo, A. Alberti, M. Guerra, *Macromolecules* **2005**, *38*, 3129.
[30] M. Destarac, D. Charmot, X. Franck, S. Z. Zard, *Macromol. Rapid Commun.* **2000**, *21*, 1035.
[31] A. Goto, K. Sato, Y. Tsujii, T. Fukuda, G. Moad, E. Rizzardo, S. H. Thang, *Macromolecules* **2001**, *34*, 402.
[32] M. Mertoglu, A. Laschewsky, K. Skrabania, C. Wieland, *Macromolecules* **2005**, *38*, 3601.
[33] G. Moad, J. Chiefari, Y. K. Chong, J. Krstina, R. T. A. Mayadunne, A. Postma, E. Rizzardo, S. H. Thang, *Polym. Int.* **2000**, *33*, 993.
[34] S. Perrier, P. Takolpuckdee, C. A. Mars, *Macromolecules* **2005**, *38*, 2033.
[35] P. Takolpuckdee, C. A. Mars, S. Perrier, S. J. Archibald, *Macromolecules* **2005**, *38*, 1057.
[36] D. J. Pan, J. L. Turner, Wooley, K. L. , *Macromolecules* **2004**, *37*, 7109.
[37] R. Huisgen, *Angew. Chem.* **1968**, *80*, 329; *Angew. Chem. Int. Ed. Engl.* **1968**, *7*, 321.
[38] H. C. Kolb, M. G. Finn, K. B. Sharpless, *Angew. Chem.* **2001**, *113*, 2056; *Angew. Chem. Int. Ed.* **2001**, *40*, 2004.
[39] V. V. Rostovtsev, L. G. Green, V. V. Fokin, K. B. Sharpless, *Angew. Chem.* **2002**, *114*, 2708; *Angew. Chem. Int. Ed.* **2002**, *41*, 2596.
[40] C. W. Tornoe, C. Christensen, M. Meldal, *J. Org. Chem.* **2002**, *67*, 3057.
[41] Q. Wang, T. R. Chan, R. Hilgraf, V. V. Fokin, K. B. Sharpless, M. G. Finn, *J. Am. Chem. Soc.* **2003**, *125*, 3192.
[42] T. S. Seo, Z. M. Li, H. Ruparel, J. Y. Ju, *J. Org. Chem.* **2003**, *68*, 609.
[43] R. Manetsch, A. Krasinski, Z. Radic, J. Raushel, P. Taylor, K. B. Sharpless, H. C. Kolb, *J. Am. Chem. Soc.* **2004**, *126*, 12809.
[44] A. J. Link, D. A. Tirrell, *J. Am. Chem. Soc.* **2003**, *125*, 11164.
[45] L. V. Lee, M. L. Mitchell, S. J. Huang, V. V. Fokin, K. B. Sharpless, C. H. Wong, *J. Am. Chem. Soc.* **2003**, *125*, 9588.
[46] B. Parrish, R. B. Breitenkamp, T. Emrick, *J. Am. Chem. Soc.* **2005**, *127*, 7404.
[47] M. Malkoch, K. Schleicher, E. Drockenmuller, C. J. Hawker, T. P. Russell, P. Wu, V. V. Fokin, *Macromolecules* **2005**, *38*, 3663.
[48] Z. Zhou, C. J. Fahrni, *J. Am. Chem. Soc.* **2004**, *126*, 8862.
[49] N. V. Tsarevsky, B. S. Sumerlin, K. Matyjaszewski, *Macromolecules* **2005**, *38*, 3558.
[50] A. E. Speers, B. F. Cravatt, *Chem. Biol.* **2004**, *11*, 535.
[51] D. B. Ramachary, C. F. I. Barbas, *Chem. Eur. J.* **2004**, *10*, 5323.
[52] J. A. Opsteen, J. C. M. van Hest, *Chem. Commun.* **2005**, 57.
[53] A. J. Link, M. K. S. Vink, D. A. Tirrell, *J. Am. Chem. Soc.* **2004**, *126*, 10598.
[54] W. G. Lewis, F. G. Magallon, V. V. Fokin, M. G. Finn, *J. Am. Chem. Soc.* **2004**, *126*, 9152.
[55] B. Helms, J. L. Mynar, C. J. Hawker, J. M. J. Frechet, *J. Am. Chem. Soc.* **2004**, *126*, 15020.
[56] M. J. Joralemon, R. K. O'Reilly, C. J. Hawker, K. L. Wooley, *J. Am. Chem. Soc.* **2005**, *127*, 16892.
[57] R. K. O'Reilly, M. J. Joralemon, K. L. Wooley, C. J. Hawker, *Chem. Mater.* **2005**, *17*, 5976.
[58] G. Mantovani, V. Ladmiral, L. Tao, D. M. Haddleton, *Chem. Commun.* **2005**, 2089.
[59] N. V. Tsarevsky, K. V. Bernaerts, B. Dufour, Du F. E. Prez, K. Matyjaszewski, *Macromolecules* **2004**, *37*, 9308.
[60] G. R. Madhavan, V. Balraju, B. Mallesham, R. Chakrabarti, V. B. Lohray, *Bioinorg. Med. Chem. Lett.* **2003**, *13*, 2547.
[61] K. Sivakumar, F. Xie, B. M. Cash, S. Long, H. N. Barnhill, Q. Wang, *Org. Lett.* **2004**, *6*, 4603.
[62] D. J. Yee, V. Balsanek, D. Sames, *J. Am. Chem. Soc.* **2004**, *126*, 2282.
[63] M. S. Schiedel, C. A. Briehn, P. Bauerle, *Angew. Chem.* **2001**, *113*, 4813; *Angew. Chem. Int. Ed.* **2001**, *40*, 4677.
[64] T. Ishizone, A. Hirao, S. Nakahama, T. Kakuchi, K. Yokota, K. Tsuda, *Macromolecules* **1991**, *24*, 5230.
[65] T. Ishizone, G. Uehara, A. Hirao, S. Nakahama, K. Tsuda, *Macromolecules* **1998**, *31*, 3764.
[66] K. Tsuda, W. Hirahata, K. Yokota, T. Kakuchi, T. Ishizone, A. Hirao, *Polym. Bull.* **1997**, *53*, 173.
[67] F. Bertini, G. Audisio, J. Kiji, M. Fujita, *J. Anal. Appl. Pyrol.* **2003**, *68*, 61.
[68] K. Tsuda, T. Ishizone, A. Hirao, S. Nakahama, *Macromolecules* **1993**, *26*, 6985.
[69] L. B. Sessions, L. A. Miinea, K. D. Ericson, D. S. Glueck, R. B. Grubbs, *Macromolecules* **2005**, *38*, 2116.
[70] L. A. Miinea, L. B. Sessions, K. D. Ericson, D. S. Glueck, R. B. Grubbs, *Macromolecules* **2004**, *37*, 8967.
[71] Q. G. Ma, K. L. Wooley, *J. Polym. Sci. Polym. Chem.* **2000**, *38*, 4805.
[72] V. Butun, M. Vamvakaki, N. C. Billingham, S. P. Armes, *Polymer* **2000**, *41*, 3173.
[73] C. S. Patrickios, W. R. Hertler, N. L. Abbott, T. A. Hatton, *Macromolecules* **1994**, *27*, 2364.
[74] J. E. Kearns, C. D. McLean, D. H. Solomon, *J. Macromol. Sci. Chem.* **1974**, *A8*, 673.
[75] A. B. Lowe, N. C. Billingham, S. P. Armes, *Macromolecules* **1998**, *31*, 5991.
[76] W. R. Hertler, D. Y. Sogah, F. A. Raymond, R. D. Bauer, C. T. Chang, G. N. Taylor, L. E. Stillwagon, *Makromol. Chem. Macromol. Symp.* **1992**, 64, 137.
[77] H. E. Simmons, W. R. Hertler, B. B. Sauer, *J. Appl. Polym. Sci.* **1994**, *52*, 727.
[78] F. A. Raymond, W. R. Hertler, *J. Imaging Sci. Technol.* **1992**, 36, 243.
[79] W. R. Hertler, US patent, No. 5072029, **1991**.
[80] S. Perrier, P. Takolpuckdee, J. Westwood, D. M. Lewis, *Macromolecules* **2004**, *37*, 2709.
[81] E. J. Corey, T. K. Schaaf, W. Huber, U. Koelliker, N. M. Weinshenker, *J. Am. Chem. Soc.* **1970**, *92*, 397.
[82] K. F. Bernady, M. B. Floyd, J. F. Poletto, M. J. Weiss, *J. Org. Chem.* **1979**, *44*, 1438.
[83] D. Benoit, V. Chaplinski, R. Braslau, C. J. Hawker, *J. Am. Chem. Soc.* **1999**, *121*, 3904.
[84] K. B. Thurmond, T. Kowalewski, K. L. Wooley, *J. Am. Chem. Soc.* **1997**, *119*, 6656.
[85] H. C. Kolb, K. B. Sharpless, *Drug Discovery Today* **2003**, *8*, 1128.
[86] D. D. Diaz, S. Punna, P. Holzer, A. K. McPherson, K. B. Sharpless, V. V. Fokin, M. G. Finn, *J. Polym. Sci. Polym. Chem.* **2004**, *42*, 4392.
[87] P. Wu, A. K. Feldman, A. K. Nugent, C. J. Hawker, A. Scheel, B. Voit, J. Pyun, J. M. J. Frechet, K. B. Sharpless, V. V. Fokin, *Angew. Chem.* **2004**, *116*, 4018; *Angew. Chem. Int. Ed.* **2004**, *43*, 3928.
[88] T. Lummerstorfer, H. Hoffmann, *J. Phys. Chem. B* **2004**, *108*, 3963.
[89] J. P. Collman, N. K. Devaraj, C. E. D. Chidsey, *Langmuir* **2004**, *20*, 1051.
[90] M. J. Joralemon, K. S. Murthy, E. E. Remsen, M. L. Becker, K. L. Wooley, *Biomacromolecules* **2004**, *5*, 903.
[91] S. Takahashi, Y. Kuroyama, K. Sonogashira, N. Hagihara, *Synthesis* **1980**, 627.
[92] R. Gujadhur, D. Venkataraman, J. T. Kintigh, *Tetrahedron Lett.* **2001**, *42*, 4791.

Received: April 4, 2006
Published online: June 26, 2006

